Preparation of Low-Resistivity Ga-Doped ZnO Epitaxial Films from Aqueous Solution Using Flow Reactor

Masao Miyake, Hiroshi Fukui,* Toshiya Doi, and Tetsuji Hirato*,z

Graduate School of Energy Science, Kyoto University, Yoshida-honmachi, Sakyo-ku, Kyoto 606-8501, Japan

An aqueous process based on a unique flow-reactor design was developed for the preparation of gallium-doped ZnO (ZnO:Ga) epitaxial films with a low electrical resistivity. In this process, a ZnO:Ga film was grown on a ZnO-seeded sapphire substrate heated at 80°C under a constant flow of a reaction solution. The Ga content of the resulting films was found to increase in relation to the concentration of $GaCl_3$ used–0 to 9 mM $GaCl_3$–resulting in epitaxial growth of ZnO containing 0–5% Ga, whereas a polycrystalline ZnO film was produced with 10 mM $GaCl_3$. The electrical resistivity of the as-grown ZnO:Ga films varied from 0.2 to 2 Ω cm, but was reduced by two to three orders of magnitude after the films were annealed in air at 300°C. Thus, the lowest resistivity of 7×10^{-4} Ω cm was obtained with an annealed film containing 2.5% Ga, whose carrier concentration and mobility were 7×10^{20} cm^{-3} and 13 cm^2 V^{-1} s^{-1}, respectively. Furthermore, even though the non-doped ZnO film was rendered translucent by annealing, ZnO:Ga films with 1.8–4.0% Ga still exhibited transmittance as high as ∼80% in the visible spectrum.
© The Author(s) 2014. Published by ECS. This is an open access article distributed under the terms of the Creative Commons Attribution Non-Commercial No Derivatives 4.0 License (CC BY-NC-ND, http://creativecommons.org/licenses/by-nc-nd/4.0/), which permits non-commercial reuse, distribution, and reproduction in any medium, provided the original work is not changed in any way and is properly cited. For permission for commercial reuse, please email: oa@electrochem.org. [DOI: 10.1149/2.0321414jes]
All rights reserved.

Manuscript submitted August 11, 2014; revised manuscript received September 10, 2014. Published September 30, 2014.

Zinc oxide (ZnO) has quite promising potential for use as a transparent semiconductor in a wide variety of applications such as sensors, light-emitting diodes (LEDs), and solar cells,[1] with a number of different techniques having already been developed for the fabrication of ZnO films. Low-temperature aqueous fabrication methods have attracted particular attention, as they tend to offer greater capability to produce large-area ZnO films at minimal cost and with low environmental impact. Though often used to produce nanowires and polycrystalline films, these aqueous-solution methods can also be used to obtain epitaxial ZnO films with good electrical conductivity and high transparency.[2,3] N-type doping with group-III elements (Ga, In, or Al) to further enhance the conductivity is also feasible when using the aqueous methods.[4,5] Although there have been studies on the practical application of aqueous-synthesized ZnO films as current-spreading layers[6] or as the n-type layer in GaN-based light-emitting diodes (LEDs),[7] further improvement in the quality of such films is still needed. For instance, there is much room for improvement in terms of film conductivity, as current values still fall short of the low resistivity ($<3 \times 10^{-4}$ Ω cm) that can be obtained with more conventional vapor-phase processes.[8–13]

In aqueous synthesis, thin films are typically grown on a substrate immersed in an aqueous solution by either heating the solution or adding another reactant to induce a chemical reaction. However, using such methods means that the chemical reaction occurs in the bulk solution, resulting in not only film growth on the substrate, but also precipitation in the solution.[14,15] Furthermore, any precipitate formed can potentially settle on the growing film, thereby reducing its crystallinity and surface flatness. Any change in the concentration or pH of the solution as the reaction progresses also makes it difficult to obtain a film with high uniformity in the growth direction, or to correlate the reaction conditions with the growth mechanism and properties of the resulting film.

The problems associated with changes in the composition of the aqueous solution can be avoided by generating film growth through heating of the substrate under a constant supply of fresh reaction solution using a flow reactor.[16,17] As it is only the substrate that is heated directly, not the solution, precipitation is effectively suppressed. Furthermore, because the film is grown under more precisely controlled and constant conditions, higher-quality films can be obtained. There have been a few reports regarding the use of flow systems for the deposition of materials on substrates from aqueous solution, with Ito et al. reporting the deposition of polycrystalline ZnO[18] and CdS[19] films by flowing a heated solution over a substrate. McPeak et al. also succeeded in growing dense arrays of ZnO nanowires[16,17] and $Cd_{1-x}Zn_xS$ films[20] by chemical bath deposition using a flow microreactor. Building on this work, this paper reports the preparation of epitaxial Ga-doped ZnO (ZnO:Ga) films using an aqueous process with a flow reactor. The effects of varying the Ga ion concentration in the reaction solution on the Ga content, crystal structure, and surface morphology of the resulting ZnO:Ga films were assessed along with the electrical properties and transmittance spectra of the films, with a view toward obtaining a low resistivity and high transmittance.

Experimental

ZnO:Ga films were grown using a custom-built flow reactor, which is shown schematically in Fig. 1. The basic structure of this reactor is similar to that described in Ref 16; the polytetrafluoroethylene (PTFE) main body had an oval channel (1 × 20 × 58 mm) with a solution inlet (3 mm ϕ) at one end and an outlet at the other. The oval channel was covered by an upper plate, to which the substrate (a 5 × 7 mm single crystal of A-plane sapphire) was attached facing downwards to prevent settling of precipitates on its surface. An epitaxial ZnO seed layer, measuring ∼100 nm in thickness, was formed in advance on this substrate by pulsed laser deposition at a temperature of 700°C and oxygen pressure of 10^{-2} Pa to ensure adhesion of the ZnO film that would be deposited later. The orientation relationship between the seed layer and the substrate was [0001] ZnO // $[11\bar{2}0]$ sapphire and $[2\bar{1}\bar{1}0]$ ZnO // [0001] sapphire.[21,22] The channel was then sealed by bolting the upper plate to the main body, with a fluoro-rubber O-ring placed between them. A sheet thermocouple (MF-0-K, Toadenki K.K.) was placed on the back of the substrate, which was then heated by a ceramic heater (SDM302, 20 × 20 mm, Sakaguchi E.H Vac Corp.) affixed to the surface of the upper plate. A thermostat (TFJ-500, AS ONE Corp.) connected between the thermocouple and heater was used to control the temperature of the substrate.

The reaction solution used to grow the ZnO:Ga films in this study was prepared by dissolving an excess amount of ZnO powder in an aqueous solution comprising 0.9 M NH_3, 0.1 M NH_4NO_3, and 3 mM sodium citrate tribasic dehydrate.[23] To provide a source of Ga ions, 0–10 mM of $GaCl_3$ was added, after which the solution was equilibrated with the ZnO powder in a sealed container under agitation at room temperature (∼25°C) for more than a day. The pH of the solution was 10.8 at 25°C. Next, the solution was flowed through a filter (Satorius Stedim Biotech, 0.45 μm) to remove any solid particles. It was then sent through the reactor, using a syringe pump (YMC, YSP-101) with a constant flow rate of 90 μL min^{-1}. In

*Electrochemical Society Active Member.
zE-mail: hirato.tetsuji.2n@kyoto-u.ac.jp

Downloaded on 2015-04-01 to IP 130.54.110.71 address. Redistribution subject to ECS terms of use (see ecsdl.org/site/terms_use) unless CC License in place (see abstract).

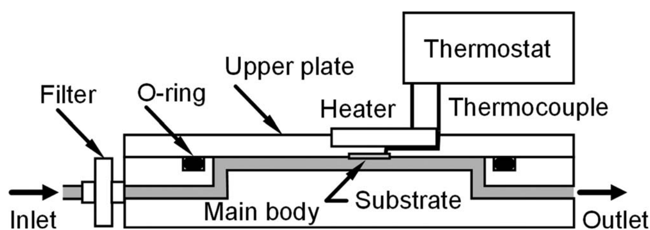

Figure 1. Schematic cross-sectional view of the flow reactor used in this study.

order to prevent the formation of bubbles on the substrate surface, a 20-psi inline back-pressure regulator (Upchurch) was installed at the outlet of the reactor.[16] By heating the substrate to 80°C at a rate of 4°C min^{-1} and then maintaining this temperature for 6 h, a ZnO:Ga film was formed. These films were then thermally annealed in air using an electric furnace (KBF848N1, Koyo Thermo Systems Co. Ltd.) by heating at 4.5°C min^{-1} to 300°C, holding at this temperature for 0.5 h, and slow cooling in the furnace.

X-ray diffraction (XRD) patterns and pole figures of the produced films were obtained using an X-ray diffractometer (X'pertPRO-MPD, PANalytical) with Cu *K*α radiation. A scanning electron microscope (SEM; JSM-6510LV, JEOL) was used to observe the surface morphology and fractured cross-sections of the films, whose thickness values were also determined. The Ga content of the ZnO films was determined by energy-dispersive X-ray spectroscopy (EDX; INCAxact, Oxford Instruments). The electrical resistivity, carrier concentration, and mobility of the films were measured with a resistivity/Hall measurement system (ResiTest 8300, Toyo Corporation) using the van der Pauw method and four 1-mm-ϕ Al electrodes formed on each film by vacuum evaporation. Finally, the transmittance of each film was measured by a spectrophotometer (UV-2450, Shimadzu).

Results and Discussion

The deposition of the ZnO:Ga films in this study was based on the fact that the solubility of ZnO in an ammonia solution decreases with increasing temperature,[24] and that when such a solution contains Ga ions, the ZnO crystals produced will incorporate Ga ions. This was confirmed by the EDX analysis of the ZnO films obtained (Fig. 2), which showed that the Ga content of the film increased by up to ∼8% with increasing $GaCl_3$ concentration in the solution. More importantly, the films grown from solutions with ≤7 mM $GaCl_3$ were colorless and transparent, whereas a solution with >7 mM $GaCl_3$ resulted in a white and translucent film. This difference in appearance is attributed to the surface morphology of the films; the SEM images in Fig. 3 show

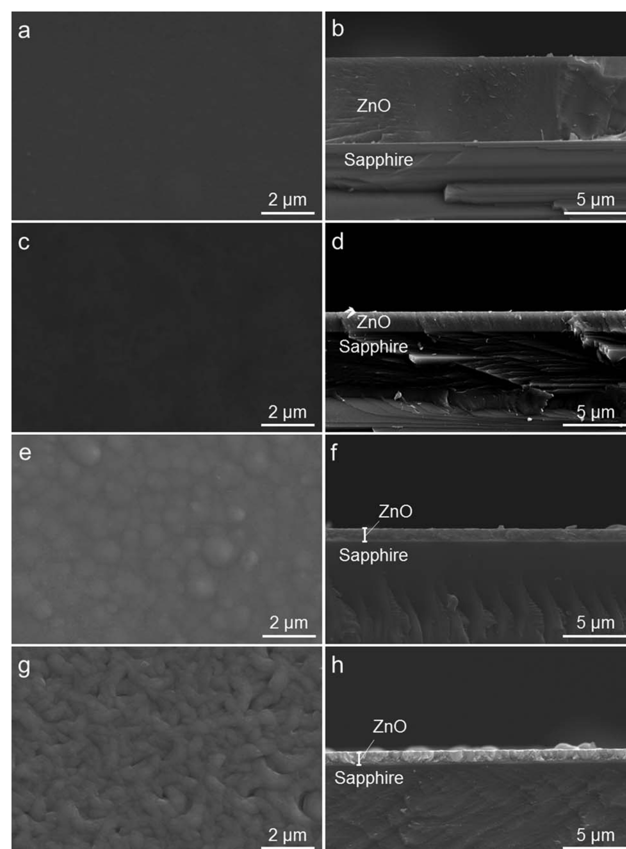

Figure 3. SEM images showing the surface and fractured cross-section of ZnO:Ga films grown from (a,b) 1, (c,d) 5, (e,f) 9, and (g,h) 10 mM $GaCl_3$ solutions. The Ga concentrations of the films were (a,b) 0.6, (c,d) 2.5, (e,f) 5.2, and (d) 8.3%.

that films with low Ga content had smooth, leveled surfaces; whereas a high Ga content resulted in a rough surface with a grain size of ∼700 nm. The formation of a rougher surface with increasing $GaCl_3$ concentration is in agreement with results reported by Le et al.[4]

Cross-sectional SEM observation revealed variations in the film thickness along the direction of the solution flow; i.e., the film became thinner further downstream of the flow reactor. This variation in thickness was at most only 15%, however. The thickness of the film was also found to be influenced by the $GaCl_3$ concentration, with Fig. 4 clearly showing decreases in film thickness with increasing

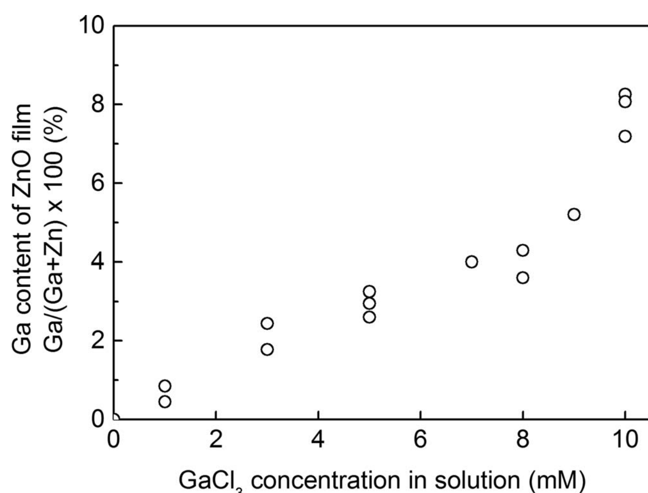

Figure 2. Ga content of ZnO films grown from solutions with various $GaCl_3$ concentrations.

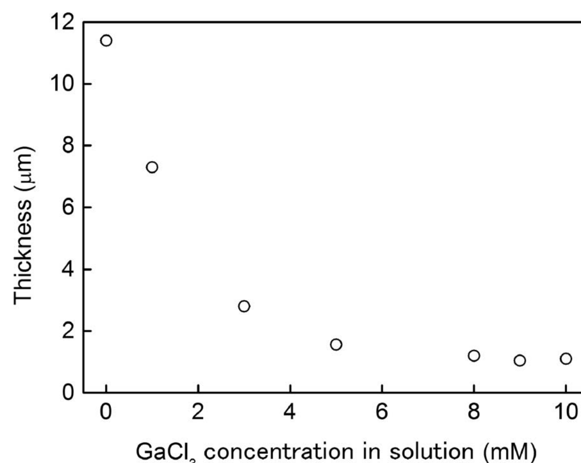

Figure 4. Thickness of ZnO:Ga films produced after 6 h of growth from solutions of various $GaCl_3$ concentrations.

Downloaded on 2015-04-01 to IP 130.54.110.71 address. Redistribution subject to ECS terms of use (see ecsdl.org/site/terms_use) unless CC License in place (see abstract).

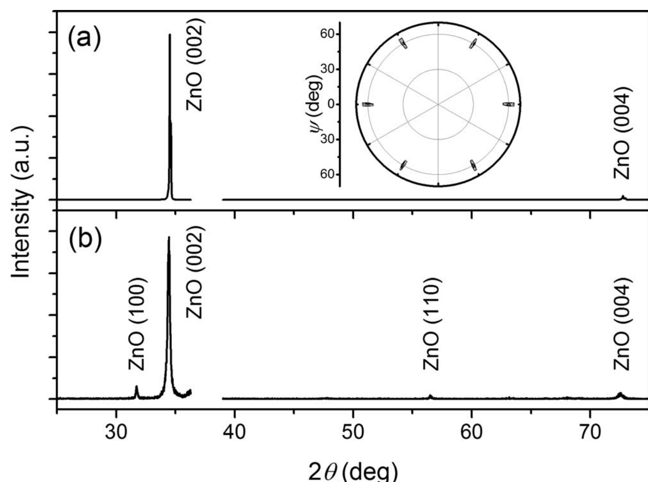

Figure 5. θ–2θ scan XRD patterns of films grown from solutions containing (a) 5 mM or (b) 10 mM $GaCl_3$. The 2θ range between 36.3° and 39.0° was not scanned so as to avoid the intense reflection from the sapphire substrate entering the counter. The inset shows a ZnO {101} pole figure of the film in (a).

$GaCl_3$ concentration. This reduction in the growth rate of ZnO:Ga was most likely caused by Ga ions (GaO_2^-) adsorbed on the surface of the growing ZnO crystal, thereby inhibiting adsorption of Zn ions onto the existing crystal. Indeed, citrate ions are known to slow the growth of ZnO in precisely this manner.[2]

In the XRD patterns, only the diffraction peaks associated with the ZnO (002) and ZnO (004) planes were detected for films grown from solutions with ≤9 mM $GaCl_3$, as shown in Fig. 5(a). The corresponding ZnO {101} pole figure reveals a clear six-fold symmetry (inset of Fig. 5(a)) that was indicative of epitaxial growth. In contrast, the 10 mM $GaCl_3$ solution produced a film that exhibited additional ZnO (100) and (110) diffraction peaks (Fig. 5(b)), suggesting polycrystalline growth. A closer look at the ZnO (002) diffraction peaks (Fig. 6) clearly reveals that the positions of the peaks shifted toward higher 2θ values; i.e., the ZnO lattice shrank in the *c*-direction as

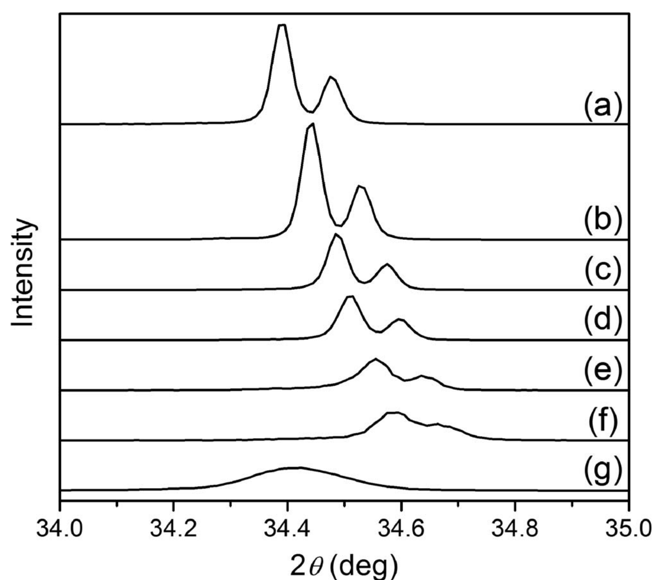

Figure 6. Enlarged XRD patterns showing ZnO (002) diffraction peaks of films grown from solutions containing (a) 0, (b) 1, (c) 3, (d) 5, (e) 7, (f) 9, or (g) 10 mM $GaCl_3$. The Ga concentrations of the films were (a) 0, (b) 0.6, (c) 1.8, (d) 2.5, (e) 4.0, (f) 5.2, and (g) 8.3%. The two peaks represent diffraction by the $K\alpha_1$ and $K\alpha_2$ lines.

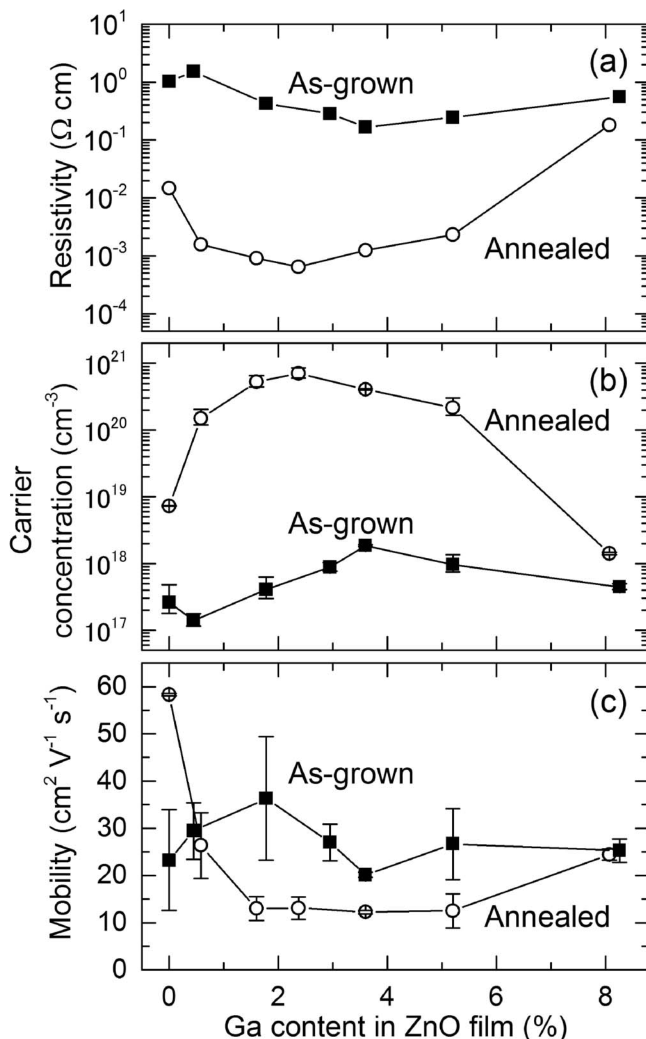

Figure 7. (a) Resistivity, (b) carrier concentration, and (c) mobility of ZnO:Ga films before and after annealing.

the $GaCl_3$ concentration was increased from 0 to 9 mM. This shrinkage can be explained by the presence of Ga in the ZnO crystal as a solid-solution, as the covalent bond length between Ga and O atoms is shorter than that between Zn and O atoms.[25] This shift in the peak position ceased when the $GaCl_3$ concentration was increased from 9 to 10 mM, returning to a pattern similar to that of the film without Ga, which suggests that Ga was deposited as a secondary phase at this concentration. The series of XRD patterns also shows that the diffraction peaks became broader as the $GaCl_3$ concentration was increased, indicating that increasing the amount of Ga incorporated in a ZnO:Ga crystal degraded its overall crystallinity.

From the electrical properties of the films shown in Fig. 7, it is evident that despite the Ga doping, the resistivity of the as-grown film was as high as 0.2–2 Ω cm (Fig. 7(a)); however, in-air annealing of a film with a Ga content of 0–6% at 300°C decreased its resistivity by more than two orders of magnitude. Thus, while the resistivity of the non-doped film was 2×10^{-2} Ω cm, the minimum resistivity obtainable with a Ga content of 2.5% was 7×10^{-4} Ω cm.

This drastic decrease in resistivity was due to the increase in carrier concentration that was observed in both non- and Ga-doped films (Fig. 7(b)), reaching a maximum of 7×10^{20} cm^{-3} at 2.5% Ga (or two orders of magnitude greater than the non-doped film). Defects in the form of Zn interstitials and O vacancies are known to be electron donors in intrinsic ZnO crystals.[1] Moreover, hydrogen atoms, which can be unintentionally incorporated in ZnO crystals during crystal

Downloaded on 2015-04-01 to IP 130.54.110.71 address. Redistribution subject to ECS terms of use (see ecsdl.org/site/terms_use) unless CC License in place (see abstract).

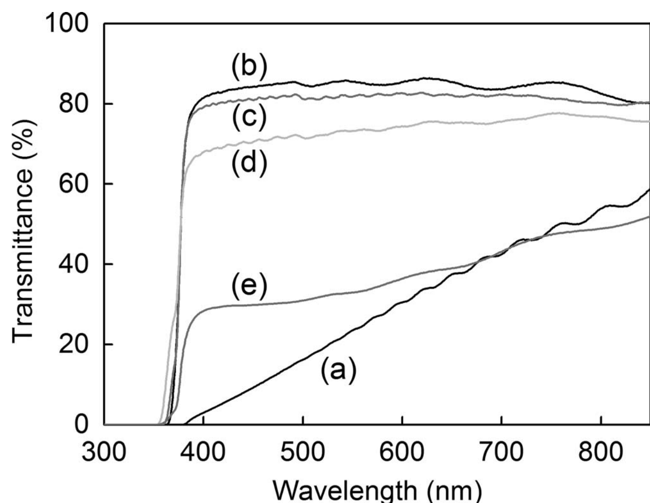

Figure 8. Transmittance spectra of films grown from solutions containing (a) 0, (b) 3, (c) 5, (d) 7, and (e) 10 mM $GaCl_3$. The Ga concentrations of the films were (a) 0, (b) 1.8, (c) 2.5, (d) 4.0, and (e) 8.3%.

growth, are believed to be dominant donors.[26] In ZnO crystals grown from aqueous solutions, hydrogen originating from hydroxide ions in the solution acts as a donor.[27] However, Ga atoms incorporated into Zn sites should be the dominant donors in a ZnO:Ga crystal. Thus, the low carrier concentration of the as-grown films indicates that most of the donor defects and impurities were either compensated by other defects or present in an electronically inactive form in the as-grown state.[27] The increase in carrier concentration with annealing is therefore attributed to the removal of compensating defects or the activation of donors, or the effect of both. As for the Ga atoms, there is the possibility that they were situated at interstitial sites in the as-grown state, but moved to substitutional Zn atom sites upon annealing.[4] At the maximum carrier concentration recorded, a simple calculation showed that about 70% of the Ga atoms in the ZnO:Ga film act as effective donors, with negligible contributions from other donors. However, further increase in the Ga content (i.e., >2.5%) reduced the carrier concentration. This is explained by the formation of compensating lattice defect complexes such as (Ga_{Zn}–$O_{interstitial}$) and (Ga_{Zn}–V_{Zn}), which were caused by the introduction of excess Ga atoms into the ZnO crystal.[4,28]

The carrier mobilities of the Ga-doped films were slightly reduced by annealing, although the value was improved for the non-doped film (Fig. 7(c)). Given that the mobility of the non-doped film after annealing was 58 $cm^2\ V^{-1}\ s^{-1}$, compared to 13 $cm^2\ V^{-1}\ s^{-1}$ for the film with 2.5% Ga, this decrease in mobility is attributed to the dominant influence of electron scattering by ionized Ga atoms in the crystal.[29]

The minimum resistivity obtained in this study is equivalent to the best previously reported values for films grown from aqueous solutions,[4,5] despite the fact the films in the present study were annealed at a lower temperature (300°C vs. 600°C). It is also comparable to, but still slightly higher than, the values obtained with films prepared by much costlier methods.[29,30] The main factor behind the higher resistivity was the two- to three-fold smaller mobility in the present films. This means that further optimization of the annealing conditions has the potential to produce even lower resistivity in films grown from low-temperature (∼80°C) solutions.

The transmittance spectra of the ZnO:Ga films after annealing are shown in Fig. 8. As demonstrated by Richardson et al.,[27] a transparent non-doped ZnO film turns translucent when annealed. This translucent appearance corresponds to the low transmittance shown in Fig. 8. In contrast, doped films containing 1.8–4.0% Ga remained transparent after annealing, as evidenced by the optical absorption edge at ∼380 nm and high transmittance at wavelengths above 380 nm. The film with the lowest resistivity (2.5% Ga) exhibited transmittance as high as ∼80% in the visible region, but the transmittance dropped when the Ga content was above 2.5% owing to the aforementioned rougher surface of the film. Indeed, films with Ga content above 4% were already translucent in the as-grown state, and therefore had transmittance below 50%. This change from a transparent to translucent film with annealing was due to the formation of pores, which scattered visible light.[27] These pores formed because the as-grown ZnO film contained water molecules and hydroxide ions originating from the reaction solution, which were expelled as water vapor upon heating. The fact that the films with 1.8–4.0% Ga remained transparent after annealing at 300°C suggests that Ga suppressed the vaporization of water from the films, thereby preventing the formation of pores and improving the films' thermal stability. This is consistent with the tendency for Ga oxide hydroxide (GaOOH) to dehydrate to form an oxide (Ga_2O_3) at temperatures higher than 400°C,[31] far above the temperature required for the dehydration of $Zn(OH)_2$ to ZnO (110–140°C).[32]

Conclusions

Gallium-doped ZnO films were successfully prepared through low-temperature aqueous synthesis using a flow reactor. The Ga content of the films was found to increase with increasing $GaCl_3$ concentration; a 0–9 mM $GaCl_3$ solution resulted in epitaxial growth of ZnO:Ga with 0–5% Ga, whereas a polycrystalline film was obtained with a 10 mM $GaCl_3$ solution. While the as-grown ZnO:Ga films had resistivities of 0.2–2 Ω cm, the figures were reduced by two to three orders of magnitude when the films were annealed at 300°C in air. Thus, the lowest resistivity of 7×10^{-4} Ω cm was achieved by annealing a ZnO film with a Ga content of 2.5%, which also produced a carrier concentration and mobility of 7×10^{20} cm^{-3} and 13 $cm^2\ V^{-1}\ s^{-1}$, respectively. Unlike the non-doped ZnO film, the ZnO:Ga films containing 1.8–4.0% Ga remained transparent after annealing, exhibiting transmittance as high as ∼80% of visible light.

References

1. L. Schmidt-Mende and J. L. MacManus-Driscoll, *Mater Today*, **10**, 40 (2007).
2. D. Andeen, J. H. Kim, F. F. Lange, G. K. L. Goh, and S. Tripathy, *Adv Funct Mater*, **16**, 799 (2006).
3. T. Hamada, A. Ito, E. Fujii, D. Chu, K. Kato, and Y. Masuda, *J Cryst Growth*, **311**, 3687 (2009).
4. H. Q. Le, S. K. Lim, G. K. L. Goh, S. J. Chua, and J. Ong, *J Electrochem Soc*, **157**, H796 (2010).
5. H. Q. Le and S. J. Chua, *J Phys D: Appl Phys*, **44**, 8 (2011).
6. A. H. Reading, J. J. Richardson, C.-C. Pan, S. Nakamura, and S. P. DenBaars, *Opt Express*, **20**, A13 (2012).
7. H. Q. Le, S. K. Lim, G. K. L. Goh, S. J. Chua, N. S. S. Ang, and W. Liu, *Appl Phys B*, **100**, 705 (2010).
8. S. M. Park, T. Ikegami, and K. Ebihara, *Thin Solid Films*, **513**, 90 (2006).
9. M. Miyazaki, K. Sato, A. Mitsui, and H. Nishimura, *Journal of Non-Cryst Solids*, **218**, 323 (1997).
10. N. Nishimoto, T. Yamamae, T. Kaku, Y. Matsuo, K. Senthilkumar, O. Senthilkumar, J. Okamoto, Y. Yamada, S. Kubo, and Y. Fujita, *J Cryst Growth*, **310**, 5003 (2008).
11. H. Agura, A. Suzuki, T. Matsushita, T. Aoki, and M. Okuda, *Thin Solid Films*, **445**, 263 (2003).
12. A. Mosbah and M. S. Aida, *J Alloy Compd*, **515**, 149 (2012).
13. X. R. Deng, H. Deng, M. Wei, and J. J. Chen, *J Mater Sci-Mater Electron*, **23**, 413 (2012).
14. A. A. C. Readigos, V. M. Garcia, O. Gomezdaza, J. Campos, M. T. S. Nair, and P. K. Nair, *Semicond Sci Tech*, **15**, 1022 (2000).
15. S. M. Pawar, B. S. Pawar, J. H. Kim, O.-S. Joo, and C. D. Lokhande, *Curr Appl Phys*, **11**, 117 (2011).
16. K. M. McPeak and J. B. Baxter, *Cryst Growth Des*, **9**, 4538 (2009).
17. K. M. McPeak and J. B. Baxter, *Ind Eng Chem Res*, **48**, 5954 (2009).
18. K. Ito and K. Nakamura, *Thin Solid Films*, **286**, 35 (1996).
19. K. Ito and K. Shiraishi, *Sol Energ Mat Sol C*, **35**, 179 (1994).
20. K. M. McPeak, B. Opasanont, T. Shibata, D. K. Ko, M. A. Becker, S. Chattopadhyay, H. P. Bui, T. P. Beebe, B. A. Bunker, C. B. Murray, and J. B. Baxter, *Chem Mater*, **25**, 297 (2013).
21. D. K. Hwang, M. S. Oh, J. H. Lim, and S. J. Park, *J Phys D Appl Phys*, **40**, R387 (2007).
22. V. Srikant, V. Sergo, and D. R. Clarke, *J Am Ceram Soc*, **78**, 1931 (1995).
23. J. J. Richardson and F. F. Lange, *Cryst Growth Des*, **9**, 2576 (2009).

Downloaded on 2015-04-01 to IP 130.54.110.71 address. Redistribution subject to ECS terms of use (see ecsdl.org/site/terms_use) unless CC License in place (see abstract).

24. J. J. Richardson and F. F. Lange, *Cryst Growth Des*, **9**, 2570 (2009).
25. X. H. Yu, J. Ma, F. Ji, Y. H. Wang, X. J. Zhang, C. F. Cheng, and H. L. Ma, *J Cryst Growth*, **274**, 474 (2005).
26. A. Janotti and C. G. Van de Walle, *Rep Prog Phys*, **72**, 120561 (2009).
27. J. J. Richardson, G. K. L. Goh, H. Q. Le, L.-L. Liew, F. F. Lange, and S. P. DenBaars, *Cryst Growth Des*, **11**, 3558 (2011).
28. H. Matsui, H. Saeki, H. Tabata, and T. Kawai, *J Electrochem Soc*, **150**, G508 (2003).
29. K. Ellmer, *J Phys D Appl Phys*, **34**, 3097 (2001).
30. Z. Yang, D. C. Look, and J. L. Liu, *Appl Phys Lett*, **94**, 072101 (2009).
31. T. Sato and T. Nakamura, *Thermochimica Acta*, **53**, 281 (1982).
32. S. V. Nistor, D. Ghica, M. Stefan, I. Vlaicu, J. N. Barascu, and C. Bartha, *J Alloy Compd*, **548**, 222 (2013).

Downloaded on 2015-04-01 to IP 130.54.110.71 address. Redistribution subject to ECS terms of use (see ecsdl.org/site/terms_use) unless CC License in place (see abstract).